Journal of Energy & Environment

Journal homepage: www.uniten.edu.my/jee

# DESIGN OF DC-DC CONVERTERS FOR ELECTRIC-BIKE'S BATTERY CHARGING STATION

Z.H. Choi*, C. L. Toh

*College of Engineering, Universiti Tenaga Nasional, 43000 Selangor, Malaysia.*

**KEYWORDS**

*Solar Photovoltaic*
*Buck converter*
*Boost converter*
*Electric-Bike*

**ABSTRACT**

Electric bike has been recognized as one of the sustainable transport in urban areas. Infrastructure planning is always a key to encourage more residents switch to use electric bikes. These infrastructures include bikeways, bike sheds, bike lifts, and most importantly a fast charging station. This paper outlines power converters design for electric-bike's battery charging station. The charging station is fully powered by solar energy. It is designed to charge two types of batteries, with different voltage rating and capacity. The charging time is set to 60 minutes for both types of batteries. The DC-DC converters design are fully discussed. The feasibility of the power converters are validated via MATLAB-Simulink software. Both converters are proven to deliver the demanded power to charge eight units of battery simultaneously with less than 1 % output voltage ripples. Simulation results are enclosed with full analysis.



## 1. INTRODUCTION

Electric-motor-powered bicycle (electric-bike) has been widely used in developed countries and urban areas with high population density [1]. The electric motor of the electric-bike is operated in response to the pedaling events on the bike. City residences are encourage to use electric-bike for travelling to work places, institutes, and city center. The main aims are to reduce the traffic congestion problems and greenhouse gas emissions. In addition, this may also reinstalled a balanced lifestyle for most of the city residents. A static shows that China, Vietnam, Netherlands, and Israel give the highest access to electric-bike [2]. It is predicted that an electric-bike will be enhanced with cycling computer and more sensors in future [3]. A cyclist performance will be closely monitored by the sensors and the electric motor may trigger-on in critical condition.

In general, electric-bike designed is customized based on its special purpose. Electric motor and batteries capacity are two major components to distinguish the application of the electric-bike [1], [4]. A wide range of electric motors rated from 100 W to 1.7 kW had been documented in literatures throughout the evolution of electric-bike. These electric motors include DC servo motor [5], switch reluctance motor [6], brushless DC motor [7], and permanent magnet synchronous motors [8]. On the other hand, four types of commonly used electric-bike batteries are Lead-Acid [1], Nickel-Metal Hydride (Ni-MH) [1], Nickel-hydrogen (Ni-H) [5], and Lithium Ion (Li-ion) [7], [9], [10]. City bicycles and distance bicycles are used for average or low speed, they may employ a 150 W electric motor. However, since the city bicycles are more frequent to stop and park for charging, a low cost Lead-Acid type battery is good enough to tour around the city. Whereas, distance bicycle is preferable to employ a Ni-MH or Ni-H battery. These type of batteries are light in weight with high energy density. Besides, mountain bicycle and freight bicycle should install with a higher torque capability electric motor. The battery size of these electric-bikes can be reduced with regenerative braking control. The kinetic energy can be recovered for longer distance travelling [6], [10].

In spite of the battery size and motor power, a high efficiency electric-bike charging station is important to ensure the performance of an electric-bike. Generally, electric-bike charging stations are grid-connected [11]. Some of these charging stations are equipped with rooftop Photovoltaic (PV) system [7], [12]. With additional PV system, energy consumption from the grid can be reduced [13]. Various type of DC-DC converters had been proposed in PV generation and charging applications which include conventional buck converter [14], current-fed dc-dc boost converter [15], full-bridge isolated dc-dc converter [12], step-up three-port DC-DC converter [16], and reconfigured dc-dc converter [17].

This paper will present a preliminary design concept of DC-DC converters for a stand-alone solar-powered electric-

*Corresponding author:
E-mail address: Jameschoi2438@gmail.com

bike charging station. The specification of the charging station are as follows:

- Eighteen units of PV modules are connected in parallel on the rooftop. The maximum power point voltage and current of each PV module are specified as 30 V and 9 A.
- Simultaneous charging of four units Lithium-ion batteries rated at 24 V and four units of Lithium-ion batteries rated at 48 V.

Two different topologies of DC-DC converters will be designed, i.e. buck converter and boost converter. The feasibility of the design is validated via MATLAB/Simulink simulation software. This paper will not include any experimental results due to the limitation of research funding.

## 2. SYSTEM DESIGN

The solar powered electric-bike's charging station is illustrated in **Fig. 1**. Ideally, eighteen units of parallel connected PV modules will supply a maximum peak current of 162 A and a nominal voltage of 30 V to charge two different rating of Li-ion batteries. **Table 1** shows the specifications of these batteries. Obviously, type-B battery would be charged up faster compare to type-A battery due to its smaller battery capacity and higher charging rate [14], [15]. Based on these requirements, two conventional dc-dc converters, namely buck converter and boost converter, are proposed to regulate the demanded battery voltage ratings at 24 V and 48 V.

The DC-DC converters design are initiated from examining the total required power to charge up four units of type-A and type-B batteries simultaneously. Then both batteries will be modeled as an *R*-load to ease the converters design. The converters must be designed in continuous current mode. Besides, the output voltage ripple of the converters must keep below 1 %; whereas the inductor current ripple is limited to less than 40%.

**Table 1.** Lithium-ion batteries specifications

| Battery Type | Nominal voltage | Capacity | Charging rate |
|---|---|---|---|
| A | 24 V | 20 Ah | 1C |
| B | 48 V | 10 Ah | 2C |

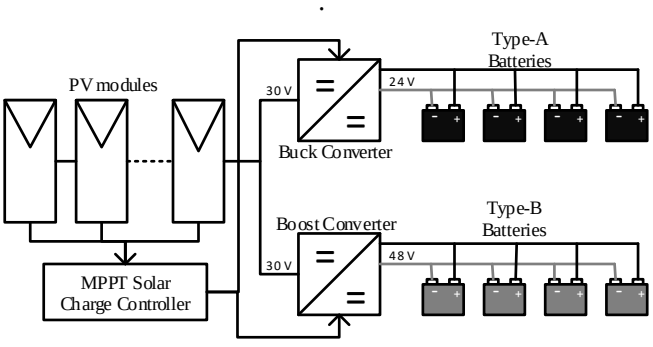


**Fig. 1.** Block diagram of solar-powered electric-bike charging system

### 2.1 Examination of Total Required Power to Charge up Type-A and Type-B Batteries Concurrently.

The required charging current and charging duration for each type of battery can be calculated using (1) and (2). **Table 2** shows the calculation results for each type of battery.

$$\textit{Charging Current, } I_c = \textit{Battery Capacity} \times \textit{Charging Rate} \quad (1)$$

$$\textit{Charging Time, } T_c = 1/(\textit{Charging Rate}) \times 60 \textit{ minutes} \quad (2)$$

Referring back to **Fig. 1**, a buck converter is needed to step down the PV source voltage from 30 V to 24 V. Assume that four units of type-A battery are configured in parallel and connected as a load to the buck converter. Hence, a total of 80 A is demanded for battery charging. On the other hand, a boost converter will be implemented for type-B battery charging. This is mainly to boost up the source voltage from 30V to 48V. Similarly, type-B batteries will also be arranged in parallel connection. Thus, a total of 40 A current will be required to charge four units of type-B battery concurrently. The total demanded power can be estimated using (3).

$$\begin{aligned} P_{total} &= P_{Batt-A} + P_{Batt-B} \\ &= \left(V_{Batt-A} \times \left(4 \times I_{C,Batt-A}\right)\right) + \left(V_{Batt-B} \times \left(4 \times I_{C,Batt-B}\right)\right) \\ &= \left(24 \times \left(4 \times 20\right)\right) + \left(48 \times \left(4 \times 10\right)\right) = 3.84kW \end{aligned} \quad (3)$$

Ideally, the PV system is assumed to produce it maximum power as in (4).

$$\begin{aligned} P_{PV} &= V_{PV} \times I_{PV} \\ &= 30 \times 162 = 4.86kW \end{aligned} \quad (4)$$

From the above calculations, the PV system is enough to cater for charging up a total of eight units Lithium-ion battery concurrently.

### 2.2 Type-A and Type-B Batteries Modelling

To ease the DC-DC converters design, both type of batteries are modelled as R-load. It is assumed that all the batteries are charged at the maximum current which are determined from the previous section. By using (5), a 24 V type-A battery is equivalent to 1.2 Ω and the 48 V type-B battery can be represented by a 4.8 Ω resistor.

$$R_{Batt-*} = V_{Batt-*} \big/ I_C \quad (5)$$

Where the asterisk symbol, *, refers to type of battery parameters to be substitute in the equation.

**Table 2.** Batteries specification and modeling for proposed power converters design

| Battery Type | $V_{Batt}$ | $I_c$ | $T_c$ | *R-load model* |
|---|---|---|---|---|
| A | 24 V | 20 A | 60 minutes | 1.2 Ω |
| B | 48 V | 10 A | 60 minutes | 4.8 Ω |

*2.3 Buck Converter Design*

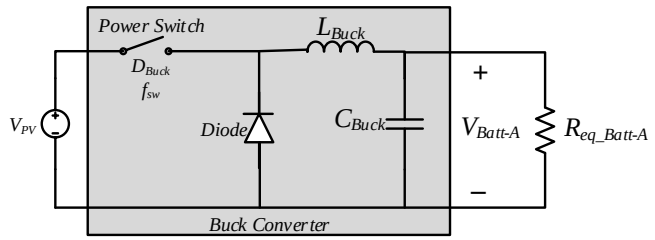


**Fig. 2.** Buck converter circuit diagram

Buck converter circuit is depicted in **Fig. 2** [16]. All the components are assumed ideal in this design. The switching frequency, $f_{sw}$, is set at 30 kHz. The duty ratio, $D_{Buck}$ of the buck converter is obtained using (6).

$$D_{Buck} = \frac{V_{Batt-A}}{V_{PV}} = \frac{24}{30} = 0.8 \tag{6}$$

As the batteries are connected in parallel, the equivalent *R*-load, can be calculated as follows:

$$\frac{1}{R_{eq\_Batt-A}} = \frac{1}{R_{Batt-A_1}} + \frac{1}{R_{Batt-A_2}} + \frac{1}{R_{Batt-A_3}} + \frac{1}{R_{Batt-A_4}} \tag{7}$$

$$R_{eq\_Batt-A} = 0.3\,\Omega$$

Hence, the minimum inductor value, $L_{min\_Buck}$ is estimated as 1 μH using (8).

$$L_{\min\_Buck} = \frac{(1-D_{Buck})R_{eq\_Batt-A}}{2f_{sw}} \tag{8}$$

To ensure the buck converter operates in continuous current mode, the inductance value is increased 10 time larger than the $L_{min\_Buck}$. Thus, 10 μH inductance ($L_{Buck}$) was used in buck converter. The output voltage ripple of the buck converter can be controlled using (9). By setting the output voltage ripple factor, $\Delta V_o / V_o$ to less than 1%, a 280 μF capacitance was implemented.

$$C_{Buck} = \frac{(1-D_{Buck})}{8L_{Buck}\left(\frac{\Delta V_o}{V_o}\right)f_{sw}^2} \tag{9}$$

*2.4 Boost Converter Design*

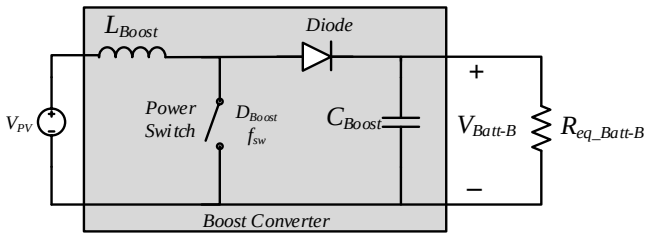


**Fig. 3.** Boost converter circuit diagram

**Fig. 3** illustrates boost converter circuit [16]. Again, all the components are assumed ideal in the design process. The switching frequency for boost converter is also set at 30 kHz. The duty cycle of the boost converter can be obtained as follows:

$$D_{Boost} = \frac{V_{Batt-B} - V_{PV}}{V_{Batt-B}} = \frac{48-30}{48} = 0.375 \tag{10}$$

Type-B batteries are configured in parallel connection, hence, the equivalent *R*-load, can be estimated using (11).

$$\frac{1}{R_{eq\_Batt-B}} = \frac{1}{R_{Batt-B_1}} + \frac{1}{R_{Batt-B_2}} + \frac{1}{R_{Batt-B_3}} + \frac{1}{R_{Batt-B_4}} \tag{11}$$

$$R_{eq\_Batt-B} = 1.2\,\Omega$$

Once the equivalent *R*-load (type-B batteries) is obtained, the minimum inductor value, $L_{min\_Boost}$ can be computed using (12).

$$L_{\min\_Boost} = \frac{D_{Boost}(1-D_{Boost})^2 R_{eq\_Batt-B}}{2f_{sw}} \tag{12}$$

The value of $L_{min\_Boost}$ is approximately 2.93 μH. To ensure continuous current mode operation, the inductance value was fixed at 15 μH in boost converter design. Equation (13) is used to determine the capacitor size.

$$C_{Boost} = \frac{D_{Boost}}{R_{eq\_Batt-B}\left(\frac{\Delta V_o}{V_o}\right)f_{sw}} \tag{13}$$

The minimum capacitance to keep the output voltage ripple below 1% is equivalent to 1.04 mF. Thus, a 2 mF capacitance was set in this design.

## 3. SIMULATION VERIFICATION & DISCUSSION

In order to verify the proposed PV charging station design, a simulation model has been developed using MATLAB/ Simulink version 2016 as shown in **Fig. 4**. The eighteen units of PV modules are modeled as a single DC source in this simulation. The source voltage is set to 30 V which is equivalent to the maximum power point voltage value. The proposed buck and boost converters are connected in parallel and supplied by the same set of PV panels (dc source). Both converters employ an IGBT as the power semiconductor to perform the high switching chopper operation. The simulations parameters of DC-DC converters are listed in **Table 3.** The 1.2 Ω resistors, R1 – R4, that connected in parallel represent type-A batteries. Meanwhile, the 4.8 Ω resistors R5 – R8 represent the type-B batteries.

**Table 3.** Simulation Parameters for the Proposed Charging Station

| | Buck Converter | Boost Converter |
|---|---|---|
| Switching Frequency, $f_{sw}$ | 30 kHz | 30 kHz |
| Duty cycle, *D* | 0.8 | 0.375 |
| Inductance, *L* | 10 μH | 15 μH |
| Capacitance, *C* | 280 μF | 2 mF |
| Resistive load, $R_{Batt*}$ | 1.2 Ω | 4.8 Ω |

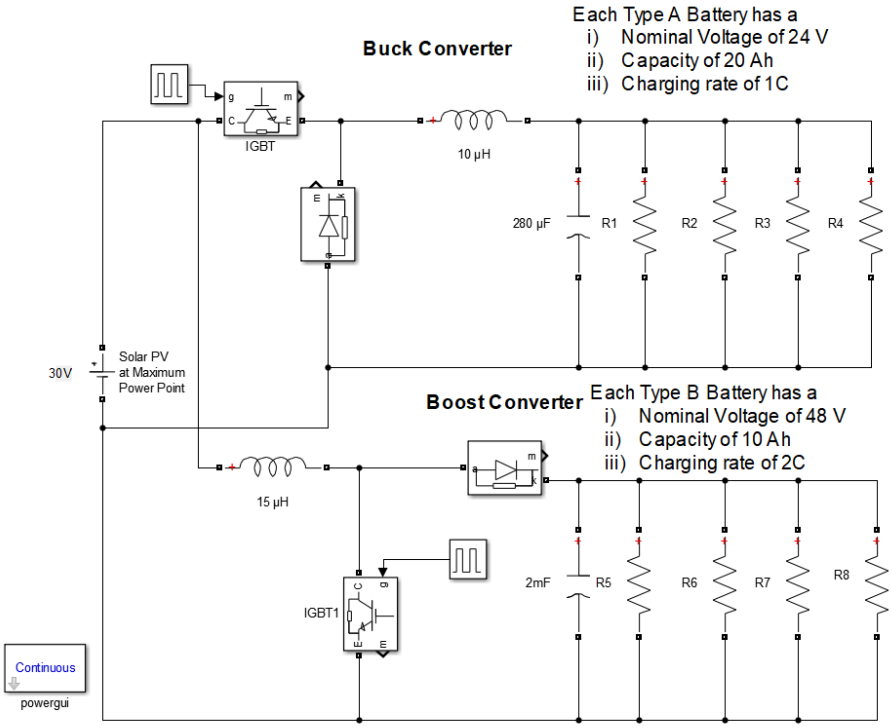


**Fig. 4.** Simulation model of power converters design for solar powered electric-bike charging station

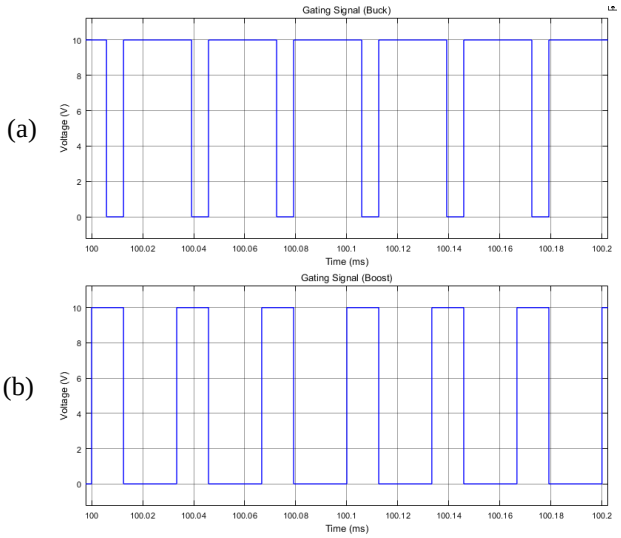


**Fig. 5.** Power switch, IGBT gating signal waveforms for (a) buck converter; (b) boost converter

**Fig. 5** shows the gating signals waveforms of the IGBT power switch for buck converter and boost converter. In buck converter, the IGBT was set to trigger with 80 % duty cycle. While the IGBT in boost converter was set to 37.5 % duty cycle. To prevent both converters drew the maximum currents at the same time, the pulse generator for buck converter was set with a phase delay of 12.5 µs. This is to ensure the PV system supplies sufficient current to charge up all the batteries concurrently. The phase delay, $\phi_{Buck}$, can be calculated as follows,

$$\phi_{Buck} = \frac{1}{f_{sw}} \times D_{Boost} \tag{14}$$

$$\phi_{Buck} = \frac{1}{30000} \times 0.375 = 12.5\ \mu s$$

**Fig. 6** shows the input source voltage and current waveforms during steady state operation. The PV source voltage waveform is shown in **Fig. 6 (a)**. The ideal dc source was constantly supplying 30 V to the buck and boost converter which were connected in parallel. As the IGBT switch of the buck converter and the inductor of the boost converter were connected directly to the dc source, a summation of these currents give the total PV current wave (**Fig. 6 (b)**). It was proved that the total current drawn from the PV system was less than 162 A. **Fig 6 (c)** illustrates the switch current waveform of the buck converter. When the IGBT was turned on the current increased linearly and reached the peak current of 87.76 A. The switch current was equal to 0 A when it was turned off. **Fig. 6 (d)** shows the inductor current of the boost converter charging and discharging repeatedly. When the IGBT switch was triggered on, PV source energy was stored in the inductance, with the inductor current raised from 51.63 A to 76.59 A. During the switch turn-off period, the energy stored in the inductance was transferred to charge up type-B batteries. Thus, inductor current reduced proportionally to the minimum value of 51.63 A.

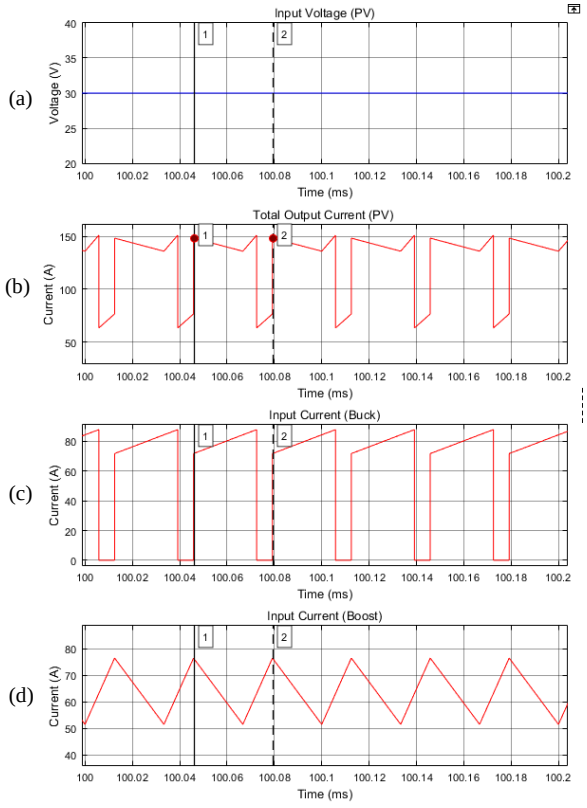


**Fig. 6.** Simulation results: (a) PV source voltage waveform; (b) PV source current waveform; (c) switch current waveform of buck converter; (d) inductor current waveform of boost converter.

**Fig. 7** presents the zoom-in view of inductor currents for both DC-DC converters. Both inductors were charging and discharging steadily. This can be proved by observing the inductor current oscillated repeatedly from 71.67 A to 87.76 A in buck converter; while the boost converter shown a current band between 51.63 A to 76.59 A. The average inductor current, $I_{L,avg}$ and the percentage of inductor current ripple, $\Delta I_L$ can be calculated using (15) and (16).

$$I_{L,avg} = I_{L,\min} + \frac{I_{L,\max} - I_{L,\min}}{2} \quad (15)$$

$$\Delta I_L = \frac{I_{L,\max} - I_{L,\min}}{I_{L,avg}} \times 100\% \quad (16)$$

Where $I_{L,min}$ indicates the minimum inductor current value. **Table 4** presents the calculation results for both converters. It is proved that both converters are operated in continuous current mode with the inductor current ripple were kept below 40%.

The zoom-in view of output voltage ripple waveforms for buck and boost converters are illustrated in **Fig. 8.** The output voltage of buck converter swings in the band of 23.95 ± 0.07 V. On the other hand, the boost converter reached a maximum output voltage, $V_{o,max}$, of 48.14 V and a minimum output voltage, $V_{o,min}$, of 47.89 V. The output voltage ripple can be calculated using (17) and (18):

$$V_{o,avg} = V_{o,\min} + \frac{V_{o,\max} - V_{o,\min}}{2} \quad (17)$$

$$\Delta V_o = \frac{V_{o,\max} - V_{o,\min}}{V_{o,avg}} \times 100\% \quad (18)$$

Both converters achieved the design requirements with the output voltage ripples are kept below 1 %.

The output current waveform of the buck converter is shown in **Fig. 9 (a)**. The buck converter is supplying approximate 80 A of current to charge up four units of type-A battery concurrently. Each unit of type-A battery receives a mean current of 19.95 A. The charging current waveform is illustrated in **Fig. 9 (b)**. Conversely, the boost converter gives 40 A of output current for type-B batteries charging operation. The output current waveform is presented in **Fig. 10 (a)**. Every single unit of type-B battery was charged up with an average current of 10 A as presented in **Fig. 10 (b)**.

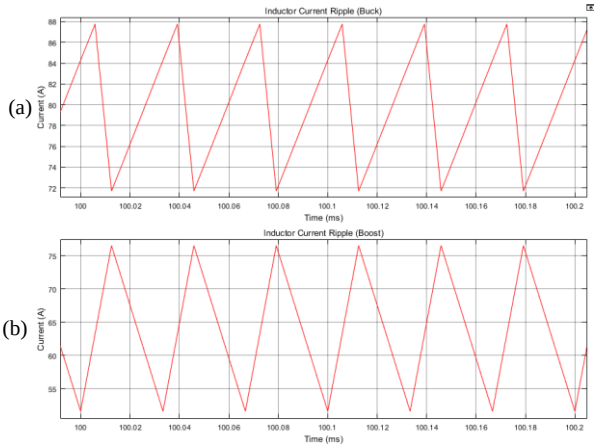


**Fig. 7.** Inductor current ripple waveforms for (a) buck converter; (b) boost converter

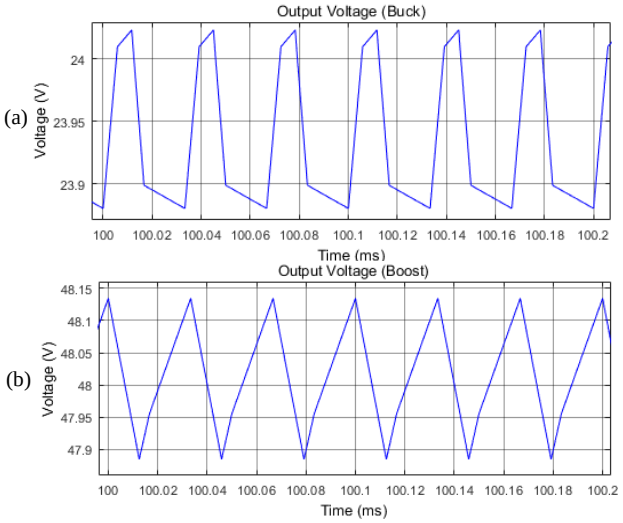


**Fig. 8.** Output voltage waveforms for (a) buck converter; (b) boost converter

**Table 4.** Proposed DC-DC converters design aspects comparison

| Converter Design Aspects | Required Specification | Buck Converter | *Boost Converter* |
|---|---|---|---|
| Minimum Inductor Current, $I_{L,min}$ | > 0 | 71.68 A | 51.63 A |
| Current mode | Continuous | Continuous | Continuous |
| Inductor Current ripple, $\Delta I_L$ | < 40 % | 20.17 % | 38.93 % |
| Output voltage ripple, $\Delta V_o$ | < 1 % | 0.60 % | 0.52 % |

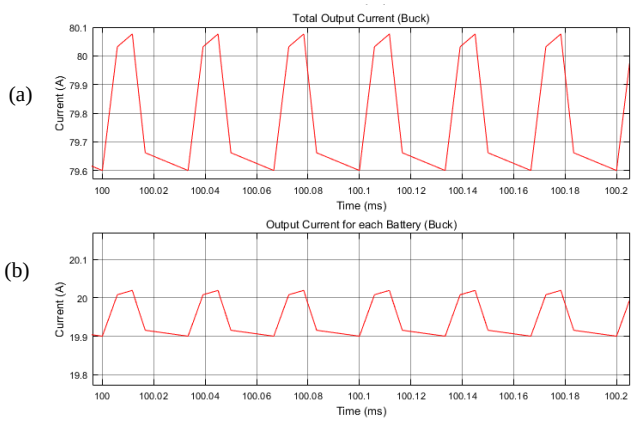


**Fig. 9.** (a) Buck converter output current waveform; (b) a single unit of type-A battery charging current waveform

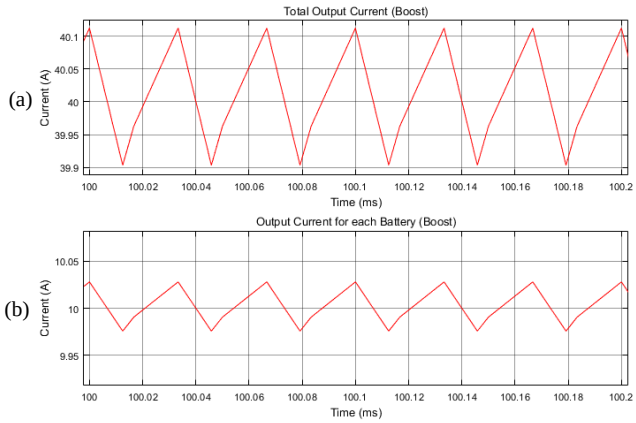


**Fig. 10.** (a) Boost converter output current waveform; (b) a single unit of type-B battery charging current waveform

## 4. CONCLUSIONS

An electric-bike fast charging station is highly demanded to promote the use of electric-bike in urban areas. This paper presents a power conversion system to charge up four units of 24 V battery and four units of 48 V battery simultaneously. The charging station is fully equipped with a series of PV panels. The charging time is limited to 60 minutes. Two different DC-DC converter topologies are proposed, namely buck and boost converters. Buck converter is a step-down DC chopper which is designed to deliver a total of 80 A charging current to charge the 24 V batteries. Whereas the boost converter will be implemented to first step-up the source voltage and supply approximate 40 A charging current to charge the 48 V batteries. The design methodology is presented with full calculation. The performance of the proposed system has been evaluated using MATLAB/ Simulink. The simulation results prove that the PV system is capable to charge up eight units of battery concurrently. Both converters are designed in continuous current mode with inductor current ripples and output voltage ripples are kept below 40% and 1% respectively. To cater for future expansion of charging demands, hybrid charging station should be considered with implementation of reconfigurable converters design.

## REFERENCES

[1] A. Muetze, Y. C. Tan, "Electric bicycles - a performance evaluation," *IEEE Industry Applications Magazine*, vol. 13, no. 4, pp. 12 - 21, 2007.

[2] A. HOLMES, "Dalia," DaliaResearch, 28 March 2017. [Online].

[3] I. Makarova, K. Shubenkova, V. Mavrin, A. Katunin, "Development of sustainable transport in smart cities," in *IEEE International Forum on Research and Technologies for Society and Industry*, Modena, Italy, 2017.

[4] G. SANCHEZ, "EVOLO," EVOLO Electric Bicycles, 2017. [Online].

[5] P.-H. Chen, "Application of Fuzzy intelligence to Elebike control design," in *The Sixth IEEE International Conference on Fuzzy Systems*, Barcelona, 1997.

[6] X. Liu, C. Liu, M. Lu, D. Liu, "Regenerative braking control strategies of switched relectance machine for electric bicycle," in *International Conference on Electric Machines and Systems*, Wuhan, China, 2008.

[7] D. Thomas, F. Vallee, V. Klonari, C. S. Ioakimidis, "Implementation of an E-bike sharing system: The effect on low voltage network using PV and smart charging station," in *International Conference on Renewable Energy Research and Applications*, Palermo, Italy, 2015.

[8] A. Christen, V. V. Haerri, "Analysis of a six- and three-phase interior permanentmagnet synchronous machine with flux concentration for an electrical bike," in *International Symposium on Power Electronics, Electrical Drives, Automation and Motion*, Ischia, Italy, 2014.

[9] S. Mesenteam, W. Feucth, A. Mittnacht, H. Frank, "Scheduling methods for smart charging of electric bikes," in *5th European Symposium on Computer Modeling and Simulation*, Madrid, Spain, 2011.

[10] O. Maier, M. Krause, S. Krauth, N. Langer, P. Pascher, J. Wrede, "Potential Benefit of Regenerative Braking on Electric Bicycles," in *IEEE International Conference on Advanced Inteligent Nechatronics*, Banff, Alberta, Canada, 2016.

[11] F. Pellitteri, V Boscaino, A. O. Di Tommaso, F. Genduso, R. Miceli, "E-bike battry charging: methods and circuits," in *International Conference on Clean Electrical Power*, Alghero, Italy, 2013.

[12] L. Celentano, D. Iannuzzi, L. Rubino, "Controller design and experimental validation of a power charging station for e-bike clever mobility," in *International Conference on Environment and Electrical Engineering*, Milan, Italy, 2017.

[13] F. Chiou, "Solar Energy for Electric Vechicles," in *IEEE Conference on Technologies for Sustainability*, Ogden, USA, 2015.

[14] M. R. Uddin, Z. Tasneem, S. I. Annie, K. M. Salim, "A high capacity synchronous buck converter for highly efficient and lightweight charger of electric easy bikes," in *International Conf. on Electrical, Computer and Communication Engineering*, Bangladash, 2017.

[15] M. Forouzesh, Y. P. Siwakoti, S. A. Gorji, F. Blaabjerg, B. Lehman, "Step-up DC-DC Converters: A comprehensive review of voltage boosting techniques, topologies and applications.," *IEEE Trans. on Power Electronics*, vol. 32, no. 12, pp. 9143-9178, 2017.

[16] Y. Chen, A. Q Huang X. Yu, "A high step-up three-port DC-DC converter for stand-alone PV/battery power systems," *IEEE. Power Electronics.* , vol. 28, no. 11, pp. 5049-5062, 2013.

[17] M. Momayyezan, B. Hredzak, V. G. Aglidis, “Integrated reconfigurable converter topology for high-voltage battery systems” *IEEE. Power Electronics.* , vol. 31, no. 3, pp. 1968-1979, 2016.

[18] "MIT Electric Vehicle Team," December 2008. [Online].

[19] D. W. Hart, Power Electronics, Indiana: McGraw Hill Education India Pvt Ltd, 2013.